^{40}Ca(d,d), (d,d'), and (d,p) Reactions with 12.8-MeV Deuterons*

H. NIEWODNICZAŃSKI, J. NURZYŃSKI, AND A. STRZALKOWSKI
Institute of Nuclear Physics, Cracow, Poland
and
Institute of Physics, Jagellonian University, Cracow, Poland

AND

G. R. SATCHLER
Oak Ridge National Laboratory, Oak Ridge, Tennesse

(Received 1 February 1966)

Differential cross sections were measured for the ^{40}Ca(d,d), (d,d'), and (d,p) reactions initiated by 12.8-MeV deuterons. Inelastic scattering to the 3.35-MeV (0^+), 3.73-MeV (3^-), and 4.48-MeV (5^-) levels of ^{40}Ca, and (d,p) reactions feeding the ground ($\frac{7}{2}^-$), 1.97-MeV ($\frac{3}{2}^-$), and 2.47-MeV ($\frac{3}{2}^-$) levels of ^{41}Ca were observed. An optical-model analysis of the elastic scattering was made, and the potentials obtained were used in a distorted-wave study of the reactions. The collective model gave a good fit to the inelastic excitation of the 3^- and 5^- levels; it was necessary to use the complex form of interaction in order to obtain reasonable values of the deformation parameters. The effects of finite range and nonlocality were included in the deuteron-stripping analysis and yield reasonable agreement with the observed cross sections. The spectroscopic factors extracted when spin-orbit coupling is included in the deuteron optical potential are significantly less than the value unity expected.

I. INTRODUCTION

THE direct-reaction processes have proven to be valuable means for getting information about the structure of atomic nuclei. While inelastic scattering of particles provide us with the parameters characterizing the collective modes of nuclear excitation, the single-particle aspects of nuclear internal motion can be studied by stripping reactions.

In the present work ^{40}Ca has been chosen as a target nucleus. The expected closed-shell character of this nucleus should give us the opportunity to study in the stripping reaction the single-particle aspects of the states of the final ^{41}Ca nucleus resulting from the addition of a single neutron to the spherical ^{40}Ca core. At the same time measurements of the differential cross sections of the inelastically scattered deuterons can give us valuable information about the collective nature of excitations of the doubly magic ^{40}Ca nucleus.

For the theoretical analysis of the experimental data the distorted-wave model has been applied. Deuteron distorting potentials are obtained from optical-model analysis of our earlier elastic-scattering data.

II. EXPERIMENTAL DATA

A. Experimental Procedure

The experimental data were obtained with a beam of 12.8-MeV deuterons from the 120-cm cyclotron of the Institute of Nuclear Physics in Caracow. A broad-range magnetic-ion spectrometer with photographic emulsions as detectors has been used for the measurements of angular distributions. The spectra of particles emitted in the reactions under consideration were taken in steps of 5° in the angular range from 10° to 110° in the laboratory system. The details of the experimental apparatus and procedure were similar to those described in our previous papers.[1,2]

The integrated beam passing through the ^{40}Ca target was collected in the Faraday cup placed behind the target and measured by means of a standard current integrator. Additional beam monitoring with two independent monitors, one viewing the Ca target and another the gold foil placed in the beam at the entrance to the scattering chamber, was also applied. An additional check for the absolute cross-section evaluation was performed by measuring the elastic scattering on gold in the Rutherford region.

The ^{40}Ca targets with a thickness of 2.28 mg/cm^2 were prepared by rolling from metallic samples and were placed immediately afterwards in the vacuum scattering chamber in order to reduce the oxygen content.

B. Results

The measured differential cross sections for inelastic scattering of deuterons exciting three excited levels of ^{40}Ca nucleus (0^+—3.35 MeV, 3^-—3.73 MeV, and 5^-—4.48 MeV) are listed in Table I, those for the ^{40}Ca(d,p) ^{41}Ca reaction leading to the ground state and two excited states (1.95 and 2.47 MeV) of the residual ^{41}Ca nucleus are shown in Table II. No significant excitation of the 3.92-MeV level of ^{40}Ca nucleus by inelastic scattering was observed.

The relative errors given in the tables include the statistical errors, inaccuracies in scanning of the emulsions, and those caused by errors in the angle setting. Because of some additional inaccuracies in the beam

* Research partly sponsored by the U. S. Atomic Energy Commission under contract with the Union Carbide Corporation.

[1] F. Pellegrini and S. Wiktor, Nucl. Phys. **41**, 412 (1963).
[2] H. Niewodniczański, J. Nurzyński, A. Strazlkowski, J. Wilczyński, P. E. Hodgson, and J. R. Rook, Nucl. Phys. **55**, 386 (1964).

TABLE I. Differential cross section for $^{40}Ca(d,d')^{40}Ca$. $E_d=12.8$ MeV. Target thickness = 2.28 mg/cm². Error of absolute value of cross section = 15%.

3.35 MeV		3.73 MeV		4.48 MeV	
$\theta_{c.m.}$ (deg)	$(d\sigma/d\Omega)_{c.m.}$ (mg/sr)	$\theta_{c.m.}$ (deg)	$(d\sigma/d\Omega)_{c.m.}$ (mb/sr)	$\theta_{c.m.}$ (deg)	$(d\sigma/d\Omega)_{c.m.}$ (mb/sr)
31.7	0.115±0.018	31.7	2.80±0.16		
36.9	0.162±0.017	37.0	3.03±0.18		
42.2	0.186±0.019	42.2	2.19±0.13	42.3	0.516±0.037
47.4	0.221±0.019	47.4	1.68±0.10	47.6	0.344±0.024
52.6	0.137±0.011	52.6	1.41±0.08	52.8	0.334±0.021
57.8	0.117±0.008	57.8	1.38±0.08	58.0	0.311±0.019
62.9	0.088±0.009	63.0	1.82±0.11	63.1	0.327±0.021
68.1	0.103±0.009	68.1	1.88±0.11	68.3	0.266±0.018
73.2	0.098±0.008	73.2	1.59±0.10	73.4	0.184±0.013
78.3	0.146±0.012	78.3	1.72±0.13	78.5	0.213±0.018
83.3	0.128±0.011	83.4	1.54±0.12	83.6	0.219±0.018
88.4	0.105±0.009	88.4	1.11±0.09	88.6	0.193±0.016
93.4	0.089±0.008	93.4	0.79±0.06	93.6	0.197±0.016
98.4	0.080±0.008	98.4	0.68±0.05	98.6	0.176±0.015
103.3	0.067±0.006	103.4	0.61±0.05	103.6	0.115±0.011
108.3	0.051±0.005	108.3	0.70±0.05	108.5	0.105±0.010
113.2	0.128±0.012	113.2	0.48±0.04	113.4	0.120±0.011

measurements and in the determination of the target thickness, the errors in the absolute values of the cross sections were estimated to be 15%.

The energy resolution of the applied detecting system (150 keV) assured sufficient separation of the groups of particles mentioned above, except for the group of protons leading to the 1.95-MeV state of the ^{41}Ca nucleus where a small admixture from the very weak level at 2.01 MeV remained unresolved.

The measurements of the elastic scattering of 12.8-MeV deuterons on ^{40}Ca nuclei published previously[3,4] were used for the optical-model analysis. Two sets of such measurements were available, taken with slightly different target thicknesses (4.6 and 5.4 mg/cm²), with two different experimental arrangements (counter telescope or magnetic spectrometer) and probably with slightly different energies. The experimental data from these two sets of measurement agree quite well, diverging only at angles larger than 90°.

TABLE II. Differential cross sections for $^{40}Ca(d,p)^{41}Ca$. $E_d=12.8$ MeV. Target thickness = 2.28 mg/cm². Error of absolute value of cross section = 15%.

Ground state		1.97 MeV		2.47 MeV	
$\theta_{c.m.}$ (deg)	$(d\sigma/d\Omega)_{c.m.}$ (mb/sr)	$\theta_{c.m.}$ (deg)	$(d\sigma/d\Omega)_{c.m.}$ (mb/sr)	$\theta_{c.m.}$ (deg)	$(d\sigma/d\Omega)_{c.m.}$ (mb/sr)
		10.3	34.9 ±2.1	10.3	13.4 ±0.87
		15.4	21.6 ±1.3	15.4	10.3 ±0.63
		20.6	13.5 ±0.81	20.6	5.74 ±0.35
		25.7	4.85 ±0.31	25.8	1.88 ±0.12
30.8	5.97±0.34	30.9	1.86 ±0.12	30.9	1.08 ±0.07
35.9	6.76±0.40	36.0	2.82 ±0.17	36.0	1.64 ±0.10
41.0	4.44±0.27	41.1	4.24 ±0.25	41.1	1.80 ±0.11
46.2	2.78±0.17	46.2	3.73 ±0.22	46.2	1.25 ±0.07
51.2	1.85±0.12	51.3	2.23 ±0.13	51.4	0.98 ±0.06
56.3	1.62±0.10	56.4	1.67 ±0.10	56.4	0.798±0.048
61.4	1.82±0.11	61.5	1.33 ±0.08	61.5	0.681±0.041
66.5	1.98±0.12	66.6	1.23 ±0.07	66.6	0.698±0.042
71.5	1.96±0.12	71.6	1.23 ±0.07	71.7	0.826±0.050
76.6	1.95±0.12	76.7	1.31 ±0.08	76.7	0.857±0.051
81.6	1.93±0.11	81.7	1.09 ±0.06	81.7	0.502±0.031
86.6	1.55±0.09	86.7	0.725±0.043	86.8	0.306±0.018
		91.7	0.602±0.036	91.8	0.221±0.014
96.6	1.20±0.08	96.7	0.568±0.034	96.8	0.305±0.018
		101.7	0.341±0.020	101.7	0.156±0.010
		106.7	0.450±0.027	106.7	0.139±0.009
		111.6	0.488±0.030	111.7	0.222±0.014

III. THEORETICAL ANALYSIS

A. Optical-Model Analysis of the Elastic Scattering

For the purpose of the present analysis, the two available sets of elastic-scattering data were combined and treated as one. The optical potential used assumes a surface-peaked absorption and has the form

$$U(r)=U_c(r)-V(e^x+1)^{-1}+4iW_D(d/dx')(e^{x'}+1)^{-1}+(\hbar/m_\pi c)^2V_s\mathbf{L}\cdot\mathbf{s}r^{-1}(d/dr)(e^x+1)^{-1}, \quad (1)$$

where

$$x=(r-r_0A^{1/3})/a, \quad x'=(r-r_0'A^{1/3})/a',$$

and $U_c(r)$ is the Coulomb potential from a uniform charge of radius $r_cA^{1/3}$. We assumed $r_c=1.3$ F. An automatic search routine[5] was used to vary the parameters of this potential so as to optimize the fit to experiment.

There are known to be considerable ambiguities in the choice of optical potentials for deuterons[6,7] and these have been examined in some detail for $^{40}Ca+d$ at other energies.[8] However, there is evidence from analysis of (d,p) reactions that the potential required is one with a real well depth $V\approx100$ MeV, and attention was restricted to this in the present work.

Previous studies[6,8] of deuteron scattering from ^{40}Ca have indicated that the imaginary potential extends to significantly larger radii than the real potential ($r_0'\approx1.5$ F while $r_0\approx1.0$F). These earlier results were used as a starting point for the present searches. The first studies were made without spin-orbit coupling, $V_s=0$. It was known from earlier work that the least well determined parameters are r_0 and a, so initially these were fixed at the value $r_0=1.0$ F and $a=0.85$ F previously found for the 12-MeV data.[8] The optimum values for the other parameters are given in Table III, denoted set No. 1. When r_0 and a are also allowed to vary, set No. 2 results; the reduction in χ^2 is only about 10%. The corresponding predicted cross sections are compared to experiment in Fig. 1.

A considerable improvement was obtained when spin-

[3] L. Freindl, H. Niewodniczański, J. Nurzyński, M. Slapa, and A. Strazalkowski, Acta Phys. Polon. **23**, 619 (1963); Institute of Nuclear Physics, Cracow, Report No. 203, 1962 (unpublished).

[4] A. Strazalkowski, Phys. Letters **2**, 121 (1962).

[5] R. M. Drisko (unpublished).

[6] E. C. Halbert, Nucl. Phys. **51**, 353 (1964); C. M. Perey and F. G. Perey, Phys. Rev. **132**, 755 (1963).

[7] R. M. Drisko, G. R. Satchler, and R. H. Bassel, Phys. Letters **5**, 347 (1963).

[8] R. H. Bassel, R. M. Drisko, G. R. Satchler, L. L. Lee, J. P. Schiffer, and B. Zeidman, Phys. Rev. **136**, B960 (1964).

orbit coupling was introduced, $V_s \neq 0$, the optimum χ^2 being reduced by more than a factor of 2. The improvement is particularly evident at the maximum around 60°. The parameters are given in Table III as set No. 3, and the comparison of theory with experiment is included in Fig. 1. The main effect of the introduction of spin-orbit coupling upon the optimum values of the other parameters is to considerably reduce the strength of the absorptive potential.

B. Inelastic Scattering

Calculations were made for the inelastic scattering to the 3.35-MeV (0^+, $l=0$), 3.73-MeV (3^-, $l=3$), and 4.48-MeV (5^-, $l=5$) states in ^{40}Ca, using the collective-model interaction and the distorted-wave approximation. Both the model and the method have been discussed in detail elsewhere[9]; suffice it to say that the inelastic angular distributions are determined once the optical-model parameters have been found by fitting the elastic scattering. The one adjustable parameter is then the deformation β_l, which is chosen to reproduce the magnitude of the measured cross section; the predicted cross sections are proportional to β_l^2.

TABLE III. Optical-model parameters.

Set	V (MeV)	r_0 (F)	a (F)	W_D (MeV)	r'_0 (F)	a' (F)	V_s (MeV)	χ^2
1	111.8	1.0	0.85	15.30	1.431	0.613	0	7.54
2	131.3	0.840	1.013	16.55	1.509	0.598	0	6.70
3	91.6	1.164	0.722	8.88	1.374	0.773	9.60	2.96

All three optical potentials described in the previous section were used. However, since the computer code was unable to include spin-orbit effects for spin-1 particles in both channels, potential No. 3 was used with $V_s=0$. (A subsidiary calculation with potential No. 3, but treating the deuteron as though it had spin $\frac{1}{2}$, showed a slight filling in of the minima in the angular distribution. It is expected that a correct spin-1 calculation would show a similar small effect.)

Two versions of the model were used, one in which only the real part of the optical potential was deformed ("real") and one in which both real and imaginary parts were deformed with the same deformation ("complex"). Figure 2 compares their predictions, for potential No. 2. It is seen that the complex coupling produces a much larger cross section (for a given β_l value) than does real coupling. As a result, using real coupling would require unacceptably large values of β_l; this effect has been noticed before for deuteron scattering.[10]

Figure 3 compares the theoretical predictions using complex coupling for potentials No. 2 and 3 with the

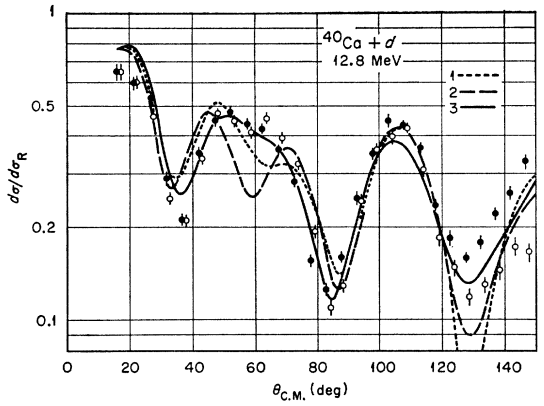

FIG. 1. Comparison of the measured cross sections for the elastic scattering of 12.8-MeV deuterons from ^{40}Ca with the predictions of the three optical potentials given in Table III. The two sets of data points correspond to targets of different thicknesses; the filled circles are for a target with 5.4 mg/cm^2, the open circles are for 4.6 mg/cm^2.

experimental data; the β_l values are given in Table IV. Excitation of the 3^- and 5^- levels by 55-MeV protons yielded[11] deformation parameters $\beta_3 \approx 0.33$ and $\beta_c \approx 0.17$, in good agreement with the values derived here. The application of the model to the 0^+ excited state is perhaps questionable. It might be regarded as a mono-

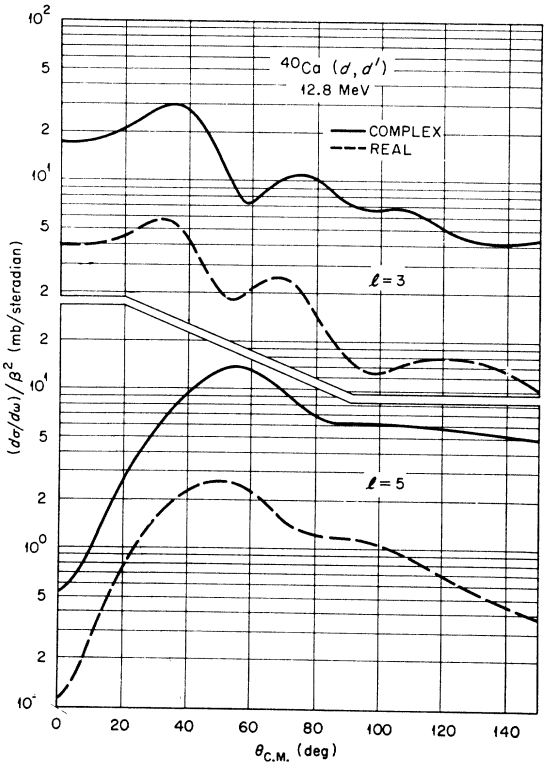

FIG. 2. Comparison of the predictions for $l=3$ and $l=5$ inelastic scattering using real and complex coupling. Potential No. 2 of Table III was used.

[9] R. H. Bassel, G. R. Satchler, R. M. Drisko, and E. Rost, Phys. Rev. **128**, 2693 (1962).

[10] J. K. Dickens, F. G. Perey, and G. R. Satchler, Nucl. Phys. **73**, 529 (1965).

[11] K. Yagi *et al.*, Phys. Letters **10**, 186 (1964).

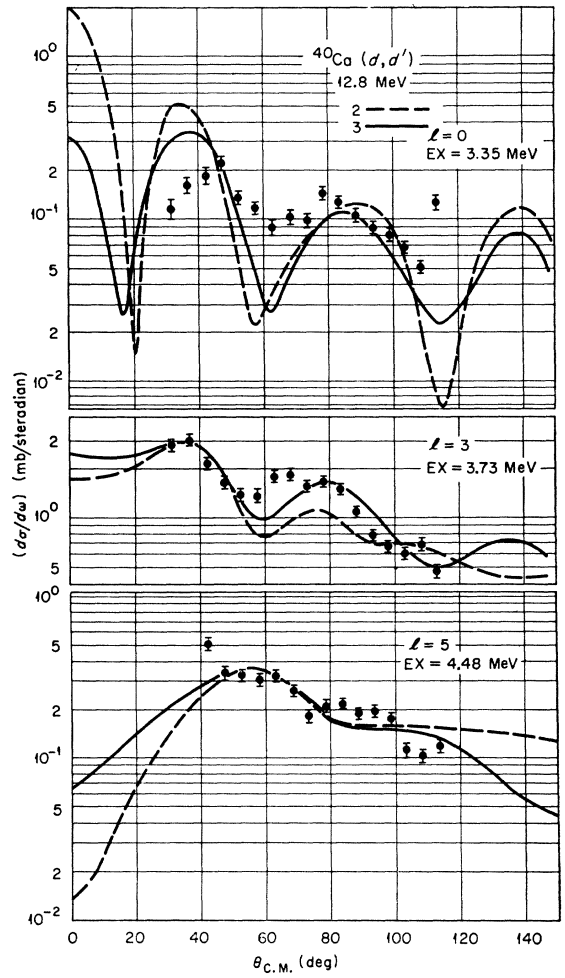

FIG. 3. Comparison of the measured inelastic cross sections for ^{40}Ca(d,d') with the predictions of potentials No. 2 and 3, using complex coupling. The deformation parameters are given in Table IV.

pole ("breathing mode") vibration, but one would expect the volume integral of the potential well to be conserved approximately during the oscillations, and this would introduce a volume interaction term additional to the surface coupling used here. There is only qualitative agreement between the measurements and the $l=0$ predictions shown in Fig. 3. The transition is quite weak, as evidenced by the small values $\beta_0 \approx 0.05$ or 0.08 required.

Potentials No. 1 and 2 give very similar predictions. The angular distributions from potential No. 3 are not very different, but the cross-section magnitudes are significantly larger. This result is due to the smaller absorptive strength of this potential (see Table III).

TABLE IV. Deformation parameters β_l.

Potential	$l=0$	$l=3$	$l=5$
2	0.08	0.32	0.16
3	0.05	0.30	0.13

C. Deuteron Stripping

The application of the distorted-wave method to the ^{40}Ca(d,p) reaction has been described and discussed in detail elsewhere.[12] For the analysis of the present data, the deuteron optical potentials described in Sec. IIA were used, but the proton optical potential and the shell-model potential into which the neutron is captured were taken to be the same as in Ref. 12. Spin-orbit coupling was included for both the neutron and proton. Corrections for finite range of the n-p interaction were made in the local energy approximation,[13] which is known to be very accurate for this reaction.[14] Although the optical potentials used were local, the damping of the wave functions in the nuclear interior which would arise from using equivalent nonlocal potentials[15] was also calculated in the local energy approximation.[13,16] The non-

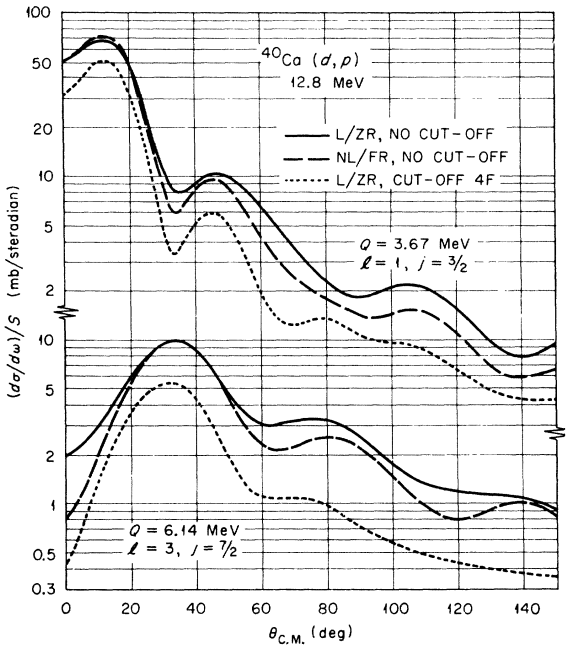

FIG. 4. Theoretical predictions for $l=1$ and $l=3$ stripping comparing the effects of nonlocality and finite-range (NL/FR) with those from the use of a radial cutoff in a local, zero-range calculation (L/ZR). Potential No. 3 was used.

[12] L. L. Lee, J. P. Schiffer, B. Zeidman, G. R. Satchler, R. M. Drisko, and R. H. Bassel, Phys. Rev. **136**, B971 (1964).

[13] F. G. Perey and D. Saxon, Phys. Letters **10**, 107 (1964), and to be published; P. J. A. Buttle and L. B. J. Goldfarb, Proc. Phys. Soc. (London) **A83**, 701 (1964).

[14] J. K. Dickens, R. M. Drisko, F. G. Perey, and G. R. Satchler, Phys. Letters **15**, 337 (1965).

[15] F. G. Perey, in *Proceedings of the Conference on Direct Interactions and Nuclear Reaction Mechanisms, Padua, 1962*, edited by E. Clementel and C. Villi (Gordon and Breach Science Publishers, Inc., New York, 1963); N. Austern, Phys. Rev. **137**, B752 (1965).

[16] S. A. Hjorth, J. X. Saladin, and G. R. Satchler, Phys. Rev. **138**, B1425 (1965).

locality range was taken to be $\beta=0.85$ F for the nucleons and $\beta=0.54$ F for the deuteron. These values assume that *all* the observed energy dependence of the optical potentials is due to nonlocality rather than any intrinsic energy variation; hence, they give an upper limit to these effects. Nonlocality reduces the contributions to the reaction amplitude from the nuclear interior by 30–40%, but it also increases the magnitude of the tail of the neutron bound-state wave function by 13% ($1f$) or 11% ($2p$). Finite range then produces an additional 10–20% reduction in the contributions from the interior. As a result, the predicted differential cross-section curves with nonlocality and finite range fall between those calculated in zero-range approximation with local potentials with and without a radial cutoff in the nuclear surface which eliminates *all* the interior contributions. This is illustrated in Fig. 4 for the $l=1$ and 3 transitions.

Calculations were made for all three deuteron potentials of Table III, including the spin-orbit coupling of No. 3. The results for potentials No. 1 and 2 were almost

TABLE V. Spectroscopic factors. Nonlocal and finite-range effects are included.

Q (MeV)	l,j	Deuteron potential No. 2	No. 3
6.14	$f_{7/2}$	0.95	0.65
4.19	$p_{3/2}$	0.44	0.34
3.67	$p_{3/2}$	0.22	0.17

identical. The experimental data are compared in Fig. 5 to the predictions of potentials 2 and 3 with nonlocal and finite-range effects included. The fits to the angular distributions are as good as those obtained at other energies[12,16]; in particular, the discrepancy remains between theory and experiment for the shape of the second maximum for the $l=3$ transition. The spectroscopic factors obtained are given in Table V. These values are not directly comparable to those obtained in Ref. 12, because nonlocality corrections were not included in that work. The effect on the tail of the neutron wave function alone would reduce all the spectroscopic factors in Ref. 12 by 22%($2p$) or 26%($1f$), but these reductions are partly compensated for by the additional damping of the contributions from the nuclear interior. The spectroscopic factors for the best potential No. 3 are significantly smaller than the values expected for a closed-shell target; one would expect the ground-state transition to have the value unity and the two $p_{3/2}$ transitions to sum to unity. A similar discrepancy for the $f_{7/2}$ state was noted at a deuteron

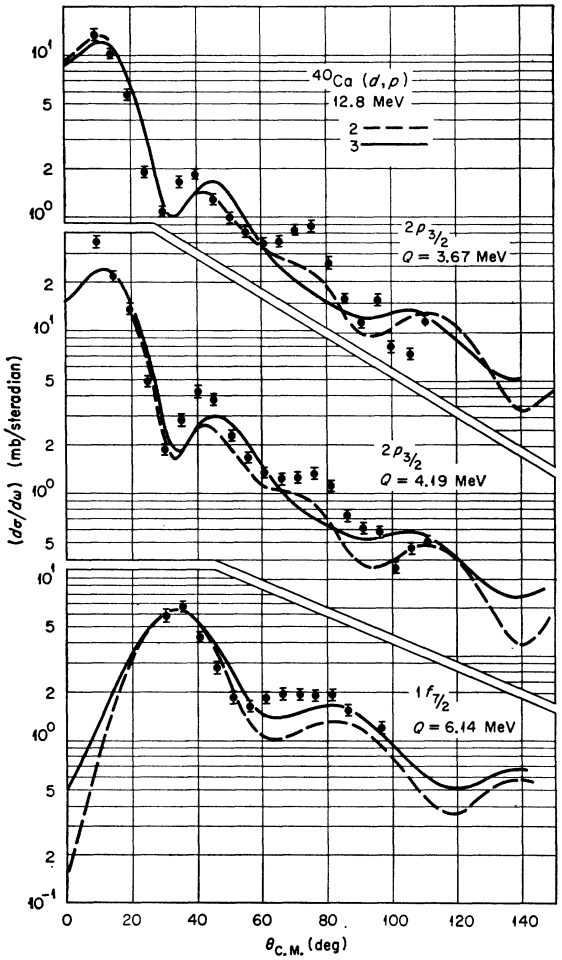

FIG. 5. Comparison of the measured cross sections for ^{40}Ca $(d,p)^{41}$Ca with the distorted-wave predictions using potentials No. 2 and 3. Nonlocality and finite-range effects are included, and no cutoff is used.

energy of 14.5 MeV.[16] The conclusions to be drawn are not clear. The results may mean ^{40}Ca does not have very pure closed-shell structure, or they may merely reflect a poor choice of parameters for the neutron potential well.[12] Another uncertainty concerns the nonlocality of the neutron potential well; we have no direct evidence on this, and we have seen that using a local potential would increase the spectroscopic factors by approximately 20%.

ACKNOWLEDGMENTS

We are indebted to R. M. Drisko for the use of the optical-model and distorted-wave codes, and to J. K. Dickens and F. G. Perey for the computation of the nonlocality and finite-range correction factors.